Inverse catalysis effect of the quark anomalous magnetic moment to chiral restoration and deconfinement phase transitions at finite baryon chemical potential

Shijun Mao*

School of Physics, Xi'an Jiaotong University, Xi'an, Shaanxi 710049, China

(Received 28 June 2022; accepted 4 August 2022; published 15 August 2022)

The effect of quark anomalous magnetic moment (AMM) to chiral restoration and deconfinement phase transitions in baryon chemical potential-temperature $(\mu_B - T)$ plane under magnetic fields is investigated in frame of a Pauli-Villars regularized Polyakov-extended Nambu-Jona-Lasinio model, which is an extension of our previous paper [Mei and Mao,Phys. Rev. D **102**, 114035 (2020)] at finite temperature and vanishing baryon chemical potential. It is found that the quark AMM plays the role of inverse catalysis to the phase transitions, and large quark AMM will change the magnetic catalysis phenomena of phase transitions to inverse magnetic catalysis in the whole $\mu_B - T$ plane. For a fixed magnetic field, the critical temperature T_c and critical baryon chemical potential μ_B^c decreases with quark AMM. The stronger the magnetic field is, the inverse catalysis effect of AMM becomes more important. For a small AMM $\kappa = \kappa_1$, it shows the magnetic catalysis effect for critical temperature T_c at vanishing μ_B with increasing magnetic field, and (inverse) magnetic catalysis effect for critical baryon chemical potential μ_B^c at vanishing T under (weak) strong magnetic field. At finite T and μ_B, there exist some crossings of the phase transition lines with different magnetic field. For a large AMM $\kappa = \kappa_2$, we obtain the inverse magnetic catalysis effect in the whole $\mu_B - T$ plane, and no crossings of phase transition lines happen.

DOI: 10.1103/PhysRevD.106.034018

I. INTRODUCTION

The study on QCD phase structure is recently extended to including external electromagnetic fields, motivated by the strong magnetic field in the core of compact stars and in the initial stage of relativistic heavy ion collisions [1–6]. From recent lattice QCD simulations with a physical pion mass, while the chiral condensate is enhanced in vacuum, the critical temperature of the chiral restoration phase transition drops down with increasing magnetic field, which is the inverse magnetic catalysis effect [7–12]. On the other hand, lattice simulations on the Polyakov loop also support the inverse magnetic catalysis for deconfinement phase transition, with a decreasing critical temperature as the magnetic field grows [11,12]. At finite baryon chemical potential, lattice QCD has the sign problem.

On analytical side, in the presence of a uniform external magnetic field $\mathbf{B} = B\mathbf{e}_z$, the energy dispersion of charged fermions takes the form $E = \sqrt{p_z^2 + 2eBl + m^2}$ with the momentum p_z along the direction of magnetic field and the Landau level $l = 0, 1, 2, \ldots$ [13]. Due to this fermion dimension reduction, almost all model calculations at mean field level report the magnetic catalysis effect both in vacuum (increasing quark mass with magnetic field) and at finite temperature (increasing critical temperature for chiral restoration and deconfinement phase transitions), see review Refs. [1,3,5,6] and the references therein. How to explain the inverse magnetic catalysis phenomena is an open question [14–41]. For a critical baryon chemical potential, people find the inverse magnetic catalysis effect at weak magnetic field, decreasing with magnetic field and accompanied with oscillations, and magnetic catalysis effect at strong magnetic field, increasing with magnetic field, see review Ref. [2] and the references therein.

The magnetic field also affects the radiative corrections of the fermion self-energy, which corresponds to the coupling between the magnetic field and the fermion anomalous magnetic moment (AMM) [42–51]. This gives rise to a new term $\frac{1}{2}\kappa_f Q_f \sigma_{\mu\nu} F^{\mu\nu}$ in the Dirac Hamiltonian, with field tensor $F^{\mu\nu}$, spin tensor $\sigma_{\mu\nu} = \frac{i}{2}[\gamma_\mu, \gamma_\nu]$ and quark electrical charge Q_f, and the coefficient κ_f is identified as the fermion AMM. The AMM term in the Hamiltonian changes the energy spectrum of fermions by removing the spin degeneracy and affects the properties of magnetized systems [39–41,51–56]. In the lowest Landau level approximation, the quark AMM κ_f reduces the effective quark mass with $m_{\text{eff}} = m - \kappa_f |Q_f B|$ and plays the role of inverse catalysis effect in the chiral restoration and deconfinement phase transitions [54,57].

*maoshijun@mail.xjtu.edu.cn

Including the AMM term, the chiral restoration and deconfinement phase transitions under external magnetic field are determined by the two competing factors, the catalysis effect of magnetic field to quark mass and inverse catalysis effect of quark anomalous magnetic moment. It is obtained that the critical temperature at vanishing baryon chemical potential increases with magnetic field for a small quark AMM, but decreases with magnetic field for a large quark AMM [52–54]. In this paper, we will study the quark AMM effect on the phase structure of chiral restoration and deconfinement in baryon chemical potential-temperature ($\mu_B - T$) plane under external magnetic field. As an extension of our previous work [54] at finite temperature and vanishing baryon chemical potential, we make use of the Polyakov-extended Nambu-Jona-Lasinio (PNJL) model [58–64]. It is found that with large enough quark AMM, the inverse magnetic catalysis phenomena will be observed in the whole $\mu_B - T$ plane.

After the introduction, we extend our PNJL framework with AMM to the finite temperature and finite baryon chemical potential case in Sec. II. The physical results and discussions are presented in Sec. III, and Sec. IV is a brief summary.

II. THE MODEL

The two-flavor PNJL model under external electromagnetic field is defined through the Lagrangian density [58–64] in chiral limit

$$\mathcal{L} = \bar{\psi}(x)\left(i\gamma^\mu D_\mu + \frac{1}{2}a\sigma^{\mu\nu}F_{\mu\nu}\right)\psi(x) + \frac{G}{2}\{[\bar{\psi}(x)\psi(x)]^2 + [\bar{\psi}(x)i\gamma_5\vec{\tau}\psi(x)]^2\} - \mathcal{U}(\Phi,\bar{\Phi}). \quad (1)$$

For the chiral section in the Lagrangian, the covariant derivative $D^\mu = \partial^\mu + iQA^\mu - i\mathcal{A}^\mu$ couples quarks to the two external fields, the magnetic field $\mathbf{B} = \nabla \times \mathbf{A}$ and the temporal gluon field $\mathcal{A}^\mu = \delta^\mu_0\mathcal{A}^0$ with $\mathcal{A}^0 = g\mathcal{A}^0_a\lambda_a/2 = -i\mathcal{A}_4$ in Euclidean space. The gauge coupling g is combined with the SU(3) gauge field $\mathcal{A}^0_a(x)$ to define $\mathcal{A}^\mu(x)$, λ_a are the Gell-Mann matrices in color space, and $Q = \mathrm{diag}(Q_u, Q_d) = \mathrm{diag}(2e/3, -e/3)$ is the quark charge matrix in flavor space. The quark AMM is introduced by the term $\frac{1}{2}a\sigma_{\mu\nu}F^{\mu\nu}$, with spin tensor $\sigma_{\mu\nu} = \frac{i}{2}[\gamma_\mu, \gamma_\nu]$, the Abel field strength tensor $F_{\mu\nu} = \partial_{[\mu}A_{\nu]}$, and the quark AMM $a = Q\kappa$ and $\kappa = \mathrm{diag}(\kappa_u, \kappa_d)$ in flavor space. G is the coupling constant in the scalar and pseudoscalar channels. The order parameter to describe chiral restoration phase transition is the chiral condensate $\langle\bar{\psi}\psi\rangle$ or the dynamical quark mass $m = -G\langle\bar{\psi}\psi\rangle$. The Polyakov potential $\mathcal{U}(\Phi,\bar{\Phi})$ is related to the Z(3) center symmetry and simulates the deconfinement [59]

$$\frac{\mathcal{U}}{T^4} = -\frac{b_2(t)}{2}\bar{\Phi}\Phi - \frac{b_3}{6}(\bar{\Phi}^3 + \Phi^3) + \frac{b_4}{4}(\bar{\Phi}\Phi)^2, \quad (2)$$

where the Polyakov loop is defined as $\Phi = (\mathrm{Tr}_c L)/N_c$ and $\bar{\Phi} = (\mathrm{Tr}_c L^\dagger)/N_c$, with $L(\mathbf{x}) = \mathcal{P}\exp[i\int_0^{1/T} d\tau \mathcal{A}_4(\mathbf{x},\tau)] = \exp[i\mathcal{A}_4/T]$. The coefficient $b_2(t) = a_0 + a_1 t + a_2 t^2 + a_3 t^3$ with $t = T_0/T$ is temperature dependent, and the other coefficients b_3 and b_4 are constants. Polyakov loop is considered as the order parameter to describe the deconfinement phase transition [58–64]. To simplify calculations, we assume a constant magnetic field $\mathbf{B} = (0, 0, B)$ along the z axis and constant quark AMM κ (or a).

Taking mean field approximation, the thermodynamic potential at finite temperature T and baryon chemical potential μ_B contains the mean field part and quark part

$$\Omega_{\mathrm{mf}} = \mathcal{U} + \frac{m^2}{2G} + \Omega_q,$$
$$\Omega_q = -\sum_{f,n,s}\int\frac{dp_z}{2\pi}\frac{|Q_f B|}{2\pi} \times [3E_f + T\ln(1+g^-) + T\ln(1+g^+)], \quad (3)$$

where

$$g^- = 3\Phi e^{-E_f^-/T} + 3\bar{\Phi}e^{-2E_f^-/T} + e^{-3E_f^-/T},$$
$$g^+ = 3\bar{\Phi}e^{-E_f^+/T} + 3\Phi e^{-2E_f^+/T} + e^{-3E_f^+/T},$$

with quark energy $E_f^\pm = E_f \pm \frac{\mu_B}{3}$, and $E_f = \sqrt{p_z^2 + \left(\sqrt{(2n+1-s\xi_f)|Q_f B| + m^2} - s\kappa_f Q_f B\right)^2}$ for flavor f, longitudinal momentum p_z, Landau level n, spin s, and sign factor $\xi_f = \mathrm{sgn}(Q_f B)$.

The ground state is determined by minimizing the thermodynamic potential, $\partial\Omega_{\mathrm{mf}}/\partial m = 0$, $\partial\Omega_{\mathrm{mf}}/\partial\bar{\Phi} = 0$, and $\partial\Omega_{\mathrm{mf}}/\partial\Phi = 0$, which leads to the three coupled gap equations for the three order parameters $m, \Phi, \bar{\Phi}$,

$$m\left(\frac{1}{2G} + \frac{\partial\Omega_q}{\partial m^2}\right) = 0, \quad (4)$$

$$\frac{\partial\mathcal{U}}{\partial\Phi} + \frac{\partial\Omega_q}{\partial\Phi} = 0, \quad (5)$$

$$\frac{\partial\mathcal{U}}{\partial\bar{\Phi}} + \frac{\partial\Omega_q}{\partial\bar{\Phi}} = 0. \quad (6)$$

From Eq. (4), we can always find a solution $m = 0$. The chiral restoration phase transition happens when nonvanishing quark mass m turns to zero. At this time, the coupled gap equations (4), (5), and (6) become decoupled. In the chiral restoration phase with $m = 0$, we only need to solve Polyakov loop Φ and $\bar{\Phi}$ from Eqs. (5) and (6). Thus, we

obtain the same critical temperature for chiral restoration and deconfinement phase transitions in chiral limit [15,54].

Because of the contact interaction among quarks, NJL models are nonrenormalizable, and it is necessary to introduce a regularization scheme to remove the ultraviolet divergence in momentum integrations. The magnetic field does not cause extra ultraviolet divergence but introduces discrete Landau levels and anisotropy in momentum space. The usually used hard/soft momentum cutoff regularization schemes do not work well in magnetic field, since the momentum cutoff together with the discrete Landau levels will cause some nonphysical results [48,52,53,65–70], such as the oscillations of chiral condensate and critical temperature, tachyonic pion mass, and the breaking of law of causality for Goldstone mode. In this work, we take into account the gauge covariant Pauli-Villars regularization scheme [15,54], where the quark momentum runs formally from zero to infinity, and the nonphysical results are cured [15,69,70]. Under the Pauli-Villars scheme, one introduces the regularized quark energy $E_f^i = \sqrt{p_z^2 + M_{\rm eff}^2 + a^i\Lambda^2}$ with $M_{\rm eff} = \sqrt{(2n+1-s\xi_f)|Q_fB| + m^2} - s\kappa_f Q_f B$ and the summation and integration $\sum_n \int dp_z/(2\pi) F(E_f)$ is replaced by $\sum_n \int dp_z/(2\pi) \sum_{i=0}^N c^i F(E_f^i)$. In our numerical calculations, all the Landau levels and longitudinal momenta are considered, and the regularization is applied to all the summations and integrations in Eqs. (3)–(6).

In chiral limit there are two parameters, the quark coupling constant G and Pauli-Villars mass parameter Λ. By fitting the pion decay constant $f_\pi = 93$ MeV and chiral condensate $\langle\bar{\psi}\psi\rangle = (-250\ \text{MeV})^3$ in vacuum, the two parameters are fixed to be $G = 7.04\ \text{GeV}^{-2}$ and $\Lambda = 1127$ MeV in Pauli-Villars scheme with number of regulated quark masses $N = 3$, and coefficients $a^1 = 1, c^1 = -3$, $a^2 = 2, c^2 = 3$, $a^3 = 3, c^3 = -1$, which are determined by constraints $a^0 = 0, c^0 = 1$, and $\sum_{i=0}^N c^i (m^2 + a^i\Lambda^2)^L = 0$ for $L = 0, 1, \ldots N-1$ [54]. For the Polyakov potential, its temperature dependence is from the lattice simulation, and the parameters are chosen as $a_0 = 6.75$, $a_1 = -1.95$, $a_2 = 2.625$, $a_3 = -7.44$, $b_3 = 0.75$, $b_4 = 7.5$, and $T_0 = 270$ MeV [59]. To evaluate the effect of quark AMM, we consider two typical sets of parameters κ, $\kappa_u^{(1)} = 0.00995\ \text{GeV}^{-1}$, $\kappa_d^{(1)} = 0.07975\ \text{GeV}^{-1}$ and $\kappa_u^{(2)} = 0.29016\ \text{GeV}^{-1}$, $\kappa_d^{(2)} = 0.35986\ \text{GeV}^{-1}$, which are phenomenologically determined by fitting the nucleon magnetic moments [48,52–54,71]. The results with vanishing AMM $\kappa_0 = 0$ are listed as comparisons.

III. RESULTS

In the lowest-Landau-level approximation, we have quark energy $E_f = \sqrt{p_z^2 + m_{\rm eff}^2}$, with effective quark mass $m_{\rm eff} = m - \kappa_f |Q_f B|$. The quark AMM affects the system through the contribution to the effective quark mass. For positive κ_f, the effective quark mass $m_{\rm eff}$ will be smaller than quark mass m, which indicates that the quark AMM induces an inverse catalysis effect to the phase transitions. In Fig. 1, we make comparison of the phase diagram with different AMM $\kappa = \kappa_0, \kappa_1, \kappa_2$ in baryon chemical potential and temperature $(\mu_B - T)$ plane at finite magnetic field $eB/m_\pi^2 = 10, 20\,(m_\pi = 134\ \text{MeV})$. With fixed magnetic field and AMM, the chiral restoration and deconfinement phase transitions happen as increasing temperature and/or baryon chemical potential, which is of first order in the whole $\mu_B - T$ plane at nonvanishing AMM. We obtain lower critical temperature and critical baryon chemical potential with larger AMM at fixed magnetic field, which demonstrates the inverse catalysis effect of quark AMM. Moreover, the inverse catalysis effect of AMM depends on the magnetic field, see the AMM term $\kappa_f|Q_fB|$ in quark energy E_f. Without a magnetic field, the phase transition lines coincide for different AMM. For stronger magnetic field, this AMM term becomes more important, and hence the separation between phase transition lines with different AMM κ becomes further.

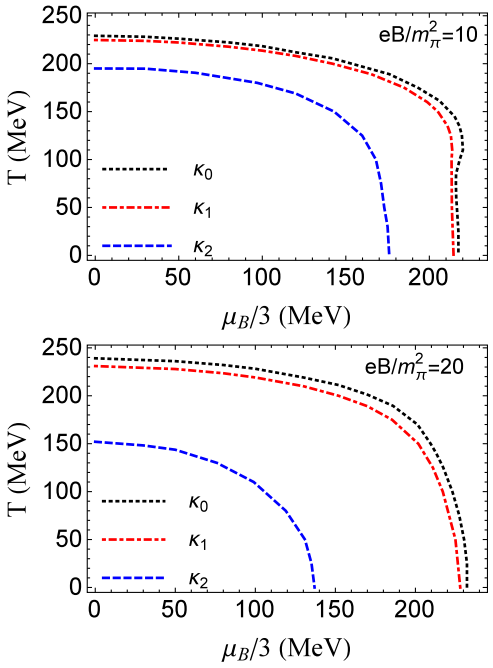

FIG. 1. The phase diagram with different AMM $\kappa = \kappa_0, \kappa_1, \kappa_2$ in baryon chemical potential and temperature $(\mu_B - T)$ plane at finite magnetic field $eB/m_\pi^2 = 10$ (upper panel) and $eB/m_\pi^2 = 20$ (lower panel).

With vanishing quark AMM $\kappa_f = 0$, the magnetic field causes the catalysis effect to the quark mass [1,3,5,6]. Including quark AMM, there appears an inverse catalysis effect caused by the term $\kappa_f|Q_fB|$. Therefore, the chiral restoration and deconfinement phase transitions under external magnetic field are controlled by the competition between the catalysis and inverse catalysis effect. First, we

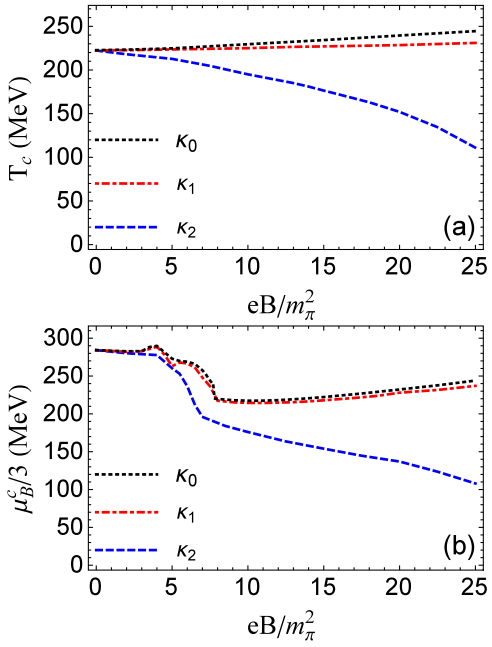

FIG. 2. The phase diagram of chiral restoration and deconfinement phase transitions in $eB-T$ and $eB-\mu_B$ plane for different quark AMM κ.

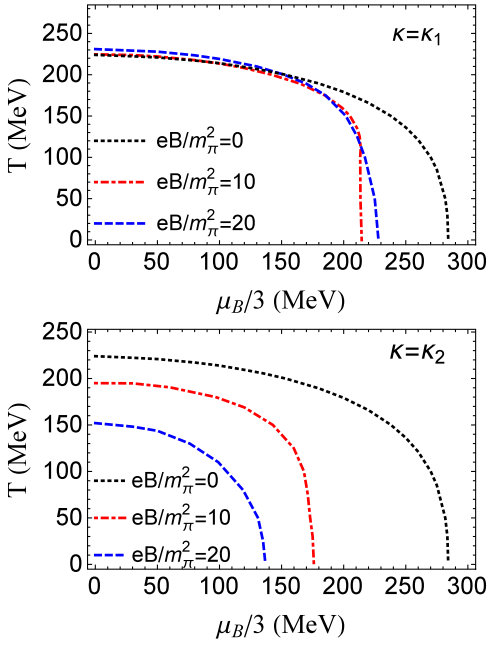

FIG. 3. The magnetic field effect on the phase structure in μ_B-T plane with fixed AMM $\kappa=\kappa_1$ (upper panel) and $\kappa=\kappa_2$ (lower panel).

discuss the magnetic catalysis and inverse magnetic catalysis phenomena for critical temperature T_c at vanishing μ_B and critical baryon chemical potential μ_B^c at vanishing T in Fig. 2, where the phase transition lines of chiral restoration and deconfinement are depicted with a fixed quark AMM $\kappa=\kappa_0,\kappa_1,\kappa_2$. Figure 2(a) is the phase diagram in $eB-T$ plane at vanishing baryon chemical potential [54]. With fixed quark AMM $\kappa=\kappa_0$, the critical temperature T_c increases with magnetic field, which is the magnetic catalysis phenomenon. For a small quark AMM $\kappa=\kappa_1$, critical temperature still increases with magnetic field, but with a slower increase ratio. For a large quark AMM $\kappa=\kappa_2$, the critical temperature decreases with magnetic field, that is the inverse magnetic catalysis phenomena. Figure 2(b) is the phase diagram in $eB-\mu_B$ plane at vanishing temperature. Without AMM, the critical baryon chemical potential μ_B^c shows inverse magnetic catalysis at a weak magnetic field, decreasing with magnetic field and accompanied with the oscillations, and magnetic catalysis at a strong magnetic field, increasing with magnetic field. The turning point is located at $eB/m_\pi^2=10$. For a small quark AMM $\kappa=\kappa_1$, critical baryon chemical potential first decreases and then increases with magnetic field, but the turning point is retarded to $eB/m_\pi^2=11$ and the oscillations are weakened. For a large quark AMM $\kappa=\kappa_2$, the critical baryon chemical potential decreases with magnetic field in the whole region, with very weak oscillations. It is the large quark AMM that changes the magnetic catalysis phenomena for T_c and μ_B^c to the inverse magnetic catalysis.

Figure 3 plots the phase structure at finite magnetic field in μ_B-T plane with fixed AMM $\kappa=\kappa_1$ (upper panel) and $\kappa=\kappa_2$ (lower panel). With a small AMM $\kappa=\kappa_1$, there exist some crossings for the phase transition lines with different magnetic fields at finite temperature and baryon chemical potential. With finite magnetic field, e.g., $eB/m_\pi^2=10$, 20, we obtain higher T_c but lower μ_B^c than $eB/m_\pi^2=0$ case. The crossing between phase transition lines with vanishing magnetic field $eB/m_\pi^2=0$ and finite magnetic field $eB/m_\pi^2=10$, 20 happens. Comparing finite magnetic field cases with $eB/m_\pi^2=10$ and $eB/m_\pi^2=20$, although we have lower T_c and μ_B^c at $eB/m_\pi^2=10$, the crossing still happens at finite temperature and baryon chemical potential. With a large AMM $\kappa=\kappa_2$, the inverse magnetic catalysis effect shows in the whole μ_B-T plane, and thus there is no crossing for the phase transition lines with different magnetic field.

IV. SUMMARY

The effect of quark AMMs to chiral restoration and deconfinement phase transitions in the μ_B-T plane under magnetic fields is investigated in frame of a Pauli-Villars regularized two-flavor PNJL model. Different from the catalysis effect of magnetic field to the quark mass, quark AMM plays the role of inverse catalysis to the phase transitions. The competition between the catalysis and inverse catalysis effect determines the chiral restoration and deconfinement phase transitions under external magnetic field. Large quark AMM will change the magnetic catalysis phenomena in phase transitions to inverse magnetic catalysis in the whole μ_B-T plane.

ACKNOWLEDGMENTS

The work is supported by the NSFC Grant No. 11775165.

[1] I. A. Shovkovy, Lect. Notes Phys. **871**, 13 (2013).
[2] F. Preis, A. Rebhan, and A. Schmitt, Lect. Notes Phys. **871**, 51 (2013).
[3] R. Gatto and M. Ruggieri, Lect. Notes Phys. **871**, 87 (2013).
[4] M. D'Elia, Lect. Notes Phys. **871**, 181 (2013).
[5] V. A. Miransky and I. A. Shovkovy, Phys. Rep. **576**, 1 (2015).
[6] J. O. Anderson and W. R. Naylor, Rev. Mod. Phys. **88**, 025001 (2016).
[7] G. S. Bali, F. Bruckmann, G. Endrődi, Z. Fodor, S. D. Katz, S. Krieg, A. Schäfer, and K. K. Szabó, J. High Energy Phys. 02 (2012) 044; Phys. Rev. D **86**, 071502 (2012).
[8] G. S. Bali, F. Bruckmann, G. Endrődi, F. Gruber, and A. Schäfer, J. High Energy Phys. 04 (2013) 130.
[9] V. Bornyakov, P. V. Buividovich, N. Cundy, O. A. Kochetkov, and A. Schäfer, Phys. Rev. D **90**, 034501 (2014).
[10] M. D'Elia, F. Manigrasso, F. Negro, and F. Sanfilippo, Phys. Rev. D **98**, 054509 (2018).
[11] G. Endrődi, J. High Energy Phys. 07 (2015) 173.
[12] G. Endrődi, M. Giordano, S. D. Katz, T. G. Kovacs, and F. Pittler, J. High Energy Phys. 07 (2019) 009.
[13] L. D. Landau and E. M. Lifshitz, *Quantum Mechanics* (Elservier Butterworth-Heinemann, London, 1938), Chap. 11.
[14] K. Fukushima and Y. Hidaka, Phys. Rev. Lett. **110**, 031601 (2013).
[15] S. J. Mao, Phys. Lett. B **758**, 195 (2016); Phys. Rev. D **94**, 036007 (2016); **97**, 011501(R) (2018); Chin. Phys. C **45**, 021004 (2021).
[16] K. Kamikado and T. Kanazawa, J. High Energy Phys. 03 (2014) 009.
[17] J. Y. Chao, P. C. Chu, and M. Huang, Phys. Rev. D **88**, 054009 (2013).
[18] F. Bruckmann, G. Endrődi, and T. G. Kovacs, arXiv:1311.3178.
[19] J. Braun, W. A. Mian, and S. Rechenberger, Phys. Lett. B **755**, 265 (2016).
[20] N. Mueller and J. M. Pawlowski, Phys. Rev. D **91**, 116010 (2015).
[21] T. Kojo and N. Su, Phys. Lett. B **720**, 192 (2013).
[22] F. Bruckmann, G. Endrodi, and T. G. Kovacs, J. High Energy Phys. 04 (2013) 112.
[23] A. Ayala, M. Loewe, A. Júlia Mizher, and R. Zamora, Phys. Rev. D **90**, 036001 (2014).
[24] A. Ayala, L. Alberto Hernández, A. Júlia Mizher, J. Cristóbal Rojas, and C. Villavicencio, Phys. Rev. D **89**, 116017 (2014).
[25] A. Ayala, C. A. Dominguez, L. Alberto Hernández, M. Loewe, and R. Zamora, Phys. Rev. D **92**, 096011 (2015).
[26] R. L. S. Farias, K. P. Gomes, G. Krein, and M. B. Pinto, Phys. Rev. C **90**, 025203 (2014).
[27] M. Ferreira, P. Costa, O. Lourenco, T. Frederico, and C. Providência, Phys. Rev. D **89**, 116011 (2014).
[28] F. Preis, A. Rebhan, and A. Schmitt, J. High Energy Phys. 03 (2011) 033.
[29] E. S. Fraga and A. J. Mizher, Phys. Rev. D **78**, 025016 (2008); Nucl. Phys. **A820**, 103C (2009).
[30] K. Fukushima, M. Ruggieri, and R. Gatto, Phys. Rev. D **81**, 114031 (2010).
[31] C. V. Johnson and A. Kundu, J. High Energy Phys. 12 (2008) 053.
[32] V. Skokov, Phys. Rev. D **85**, 034026 (2012).
[33] E. S. Fraga, J. Noronha, and L. F. Palhares, Phys. Rev. D **87**, 114014 (2013).
[34] R. Gatto and M. Ruggieri, Phys. Rev. D **82**, 054027 (2010); **83**, 034016 (2011).
[35] M. Ferreira, P. Costa, and C. Providência, Phys. Rev. D **89**, 036006 (2014).
[36] M. Ferreira, P. Costa, D. P. Menezes, C. Providência, and N. N. Scoccola, Phys. Rev. D **89**, 016002 (2014).
[37] P. Costa, M. Ferreira, H. Hansen, D. P. Menezes, and C. Providência, Phys. Rev. D **89**, 056013 (2014).
[38] A. J. Mizher, M. N. Chernodub, and E. S. Fraga, Phys. Rev. D **82**, 105016 (2010).
[39] E. J. Ferrer, V. de la Incera, I. Portillo, and M. Quiroz, Phys. Rev. D **89**, 085034 (2014).
[40] E. J. Ferrer, V. de la Incera, and X. J. Wen, Phys. Rev. D **91**, 054006 (2015).
[41] K. Xu, J. Y. Chao, and M. Huang, Phys. Rev. D **103**, 076015 (2021).
[42] J. Schwinger, Phys. Rev. **73**, 416 (1948).
[43] T. Kinoshita and B. A. Lippmann, Phys. Rev. **76**, 828 (1949).
[44] P. J. Mohr, B. N. Taylor, and D. B. Newell, Rev. Mod. Phys. **80**, 633 (2008).
[45] L. Brekke and J. L. Rosner, Comments Nucl. Part. Phys. **18**, 83 (1988).
[46] B. Jancovici, Phys. Rev. A **187**, 2275 (1969).
[47] J. P. Singh, Phys. Rev. D **31**, 1097 (1985).
[48] P. J. A. Bicudo, J. E. F. T. Ribeiro, and R. Fernandes, Phys. Rev. C **59**, 1107 (1999).
[49] E. J. Ferrer and V. de la Incera, Phys. Rev. Lett. **102**, 050402 (2009); Nucl. Phys. **B824**, 217 (2010).
[50] L. Chang, Y. X. Liu, and C. D. Roberts, Phys. Rev. Lett. **106**, 072001 (2011).
[51] E. J. Ferrer, V. de la Incera, D. M. Paret, A. P. Martínez, and A. Sanchez, Phys. Rev. D **91**, 085041 (2015).
[52] Sh. Fayazbakhsh and N. Sadooghi, Phys. Rev. D **90**, 105030 (2014).

[53] N. Chaudhuri, S. Ghosh, S. Sarkar, and P. Roy, Phys. Rev. D **99**, 116025 (2019); Eur. Phys. J. A **56**, 213 (2020); Phys. Rev. D **103**, 096021 (2021).
[54] J. Mei and S. J. Mao, Phys. Rev. D **102**, 114035 (2020).
[55] R. M. Aguirre, Phys. Rev. D **102**, 096025 (2020).
[56] Y. Y. Wang and S. Matsuzaki, Phys. Rev. D **105**, 074015 (2022).
[57] J. P. Blaizot, E. S. Fraga, and L. F. Palhares, Phys. Lett. B **722**, 167 (2013).
[58] P. N. Meisinger and M. C. Ogilvie, Phys. Lett. B **379**, 163 (1996).
[59] P. N. Meisinger, T. R. Miller, and M. C. Ogilvie, Phys. Rev. D **65**, 034009 (2002).
[60] K. Fukushima, Phys. Lett. B **591**, 277 (2004).
[61] A. Mocsy, F. Sannino, and K. Tuominen, Phys. Rev. Lett. **92**, 182302 (2004).
[62] E. Megias, E. R. Arriola, and L. L. Salcedo, Phys. Rev. D **74**, 065005 (2006).
[63] C. Ratti, M. A. Thaler, and W. Weise, Phys. Rev. D **73**, 014019 (2006); arXiv:nucl-th/0604025.
[64] S. K. Ghosh, T. K. Mukherjee, M. G. Mustafa, and R. Ray, Phys. Rev. D **73**, 114007 (2006).
[65] M. Frasca and M. Ruggieri, Phys. Rev. D **83**, 094024 (2011).
[66] Sh. Fayazbakhsh and N. Sadooghi, Phys. Rev. D **88**, 065030 (2013).
[67] T. Mandal and P. Jaikumar, Phys. Rev. C **87**, 045208 (2013); Adv. High Energy Phys. **2017**, 1 (2017).
[68] R. Z. Denke and M. B. Pinto, Phys. Rev. D **88**, 056008 (2013).
[69] S. S. Avancini, R. L. S. Farias, N. N. Scoccola, and W. R. Tavares, Phys. Rev. D **99**, 116002 (2019).
[70] B. K. Sheng, Y. Y. Wang, X. Y. Wang, and L. Yu, Phys. Rev. D **103**, 094001 (2021).
[71] M. Mekhf, Phys. Rev. D **72**, 114014 (2005).